Indian Journal of Pure & Applied Physics
Vol. 52, October 2014, pp. 708-716

High-performance current-controlled CDCCC and its applications

Pipat Prommee[1] & Fabian Khateb[2,3]

[1]Department of Telecommunications Engineering, Faculty of Engineering, King Mongkut's Institute of Technology Ladkrabang, Bangkok 10520, Thailand

[2]Department of Microelectronics, Brno University of Technology, Technická 10, Brno, Czech Republic

[3]Czech Technical University in Prague, Faculty of Biomedical Engineering, nám. Sítná 3105, Kladno, Czech Republic

E-mail: pipat@telecom.kmitl.ac.th, khateb@feec.vutbr.cz

Received 24 March 2014; revised 12 May 2014; accepted 10 July 2014

This paper presents a new high performance active element named Current Controlled Currents Differencing Current Copy Conveyer (CC-CDCCC). The main features of this element are large dynamic range, wide bandwidth and high accuracy. Furthermore, its intrinsic resistances of two input current terminals can be independently set by external balancing bias currents which lead to use low number of active elements. To demonstrate the high performance of the CC-CDCCC, two current-mode signal processing applications are presented in this paper i.e. universal filters and quadrature oscillator. Both of these applications are electronically controlled for a wide range of frequencies and they employ single CC-CDCCC and two grounded capacitors which are advantageous for monolithic integration. PSpice simulation results using the 0.25 µm CMOS technology from TSMC are included to verify the correct functionality of the proposed circuit.

Keywords: Quadrature oscillator, Universal filters, Current controlled active elements, Resistorless

1 Introduction

Electronically controlled active elements are widely used and play significant role in circuit applications. They enable tuning of specific application parameters e.g. the natural frequency and quality factor of filters or the frequency of oscillation and condition of oscillation of oscillators. Furthermore, they allow a fine-tuning in case of any possible deviations in circuit parameters after manufacturing since it is well known that the tolerance of the electronic components in monolithic integrated circuit can be unacceptably high. A variety of electronically controlled active elements have been presented in the literature[1-5], such as CCCII, CCDDCC, CCCFTA, CCCDTA and CCCDBA. In integrated circuits, realization of passive resistors on chip occupies quite large die area. Modern IC design leads to electronic resistors usage. The electronic resistors have the following benefits which are small die area and tunability feature. In practice, active elements suffer from undesirable parasitic impedances i.e. parasitic/intrinsic capacitances and resistances. However, replacing the passive resistors in circuit applications by the parasitic intrinsic resistances of the active elements become beneficial since it leads to shrink the die area of the IC and hence the total manufacturing cost. Although, the CCCDTA and CCCDBA have current controlled input intrinsic resistances, the values of these resistances are not identical and controlled by the same bias current, therefore, they could not be used for such applications that require the value of these resistance to be variant, as a result the applicability of these elements are limited.

In our survey of most recently published papers related to current-mode universal filters and quadrature oscillators we have discovered drawbacks that will be described below. Some filter applications use floating passive elements which are not suitable for integration[6,9,12]. Some filter applications lack electronic controlled feature[6,7], suffer from excessive component[6-9]. Some filters have electronic controlled feature but the balancing bias current cannot be achieved[11]. Other filter applications can use the simple feature of active building block without electronic controlled feature[10]. In recent years, the classified of active building blocks are introduced[13]. One of different active building block is a current differencing current conveyor (CDCC). It provides a differencing current output connected to a current conveyor without electronic tunability feature. The new current-mode active device named current controlled current differential current conveyor[14] was introduced with single electronic tunability but it lacks of independent tunability feature of n and p

terminals. Therefore, for implementing a second order filter or oscillator it needs at least two active elements. Regarding the quadrature sinusoidal oscillators (QSO) which are suitable for the communication system, a simple CMOS-OTA has been introduced but has no equal amplitude outputs [15]. Some oscillators use floating passive elements which are not suitable for integration[16-19], and without electronic tunability feature[20-22]. One needs 2 resistors and 3 capacitors for constructing[23] the QSO. Tunable oscillators using CDTA based on similar structure employ a grounded resistor for obtaining condition of oscillation[24,25] which is not attractive in the fully electronic tunability purpose.

Therefore, this paper presents new high-performance active element CC-CDCCC; it offers large dynamic range and wide bandwidth similar to its current-mode counterparts. The intrinsic resistances of its input current terminal are controlled independently by external bias currents. Also, two identical of intrinsic resistances can be realized by balancing two bias currents to be identical enabling a simply tuning condition of desired parameters. It enables to design for the application by using only one active element. To demonstrate the attractive features of the CC-CDCCC, in contrast to previously presented current controlled active elements, low-complexity of two current-mode applications is presented in this paper. The first application is single input multiple outputs (SIMO) universal filters and the second one is quadrature sinusoidal oscillator (QSO). Both of the applications are electronically controlled in wide range of frequencies and they employ only single CC-CDCCC and two grounded capacitors. The current output signals are obtained from current output terminals of high impedance; therefore, no additional buffers are required.

2 Current Controlled CDCCC (CC-CDCCC)

The CC-CDCCC is a new active element whose symbol and equivalent circuit are shown in Fig. 1(a and b), respectively. It has two input current terminals x_p and x_n, where their intrinsic resistances are controlled separately by two bias currents I_{Bp} and I_{Bn}, respectively. It has also a voltage input terminal y and five output current terminals z_+, z_+, z_-, p_c and n_c all of them possess high impedance values.

The characteristics of the CC-CDCC can be described as:

$$\begin{pmatrix} I_y \\ V_p \\ V_n \\ I_{z+} \\ I_{z-} \\ I_{pc} \\ I_{nc} \end{pmatrix} = \begin{pmatrix} 0 & 0 & 0 & 0 & 0 & 0 & 0 \\ 1 & R_p & 0 & 0 & 0 & 0 & 0 \\ 1 & 0 & R_n & 0 & 0 & 0 & 0 \\ 0 & 1 & -1 & 0 & 0 & 0 & 0 \\ 0 & -1 & 1 & 0 & 0 & 0 & 0 \\ 0 & 1 & 0 & 0 & 0 & 0 & 0 \\ 0 & 0 & 1 & 0 & 0 & 0 & 0 \end{pmatrix} \begin{pmatrix} V_y \\ I_p \\ I_n \\ V_{z+} \\ V_{z-} \\ V_{pc} \\ V_{nc} \end{pmatrix}. \quad \ldots(1)$$

where R_p and R_n are the intrinsic parasitic impedances of the x_p and x_n current input terminals, respectively.

The internal MOS structure of the CC-CDCCC is shown in Fig. 2. The positive and negative differential currents I_{z+} and I_{z-} can be obtained by the modified translinear current conveyors[26] (M_1-M_4 and M_9-M_{12}) with the compensated current transistors M_{15} and M_{16} and additional current mirrors. Another extra positive differential current I_{z+} is added for the circuit realization which named for both z-terminals as I_{z1+} and I_{z2+}. The currents of I_p and I_n are also duplicated to the p_c and n_c terminal by current mirrors, respectively. It should be mentioned that the number of the output current terminals of the CC-CDCCC could be arbitrarily increased simply by using the current mirror principle.

A straightforward circuit analysis of Fig. 2 leads to the following expression of the x_p terminal:

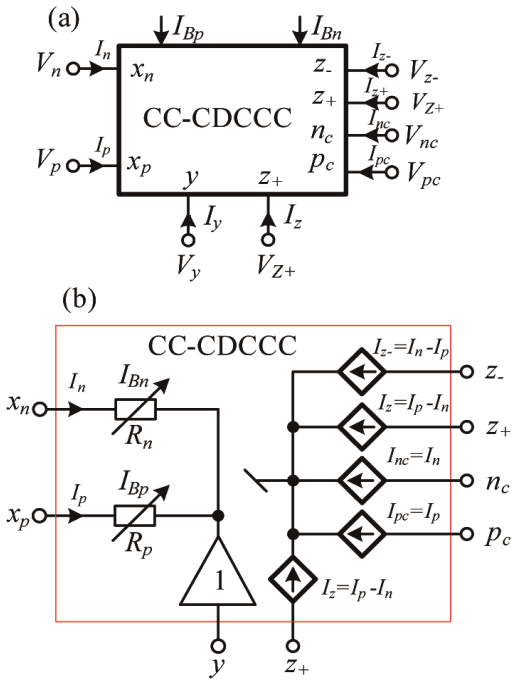

Fig. 1 — (a) Symbol of CC-CDCCC and (b) its equivalent circuit

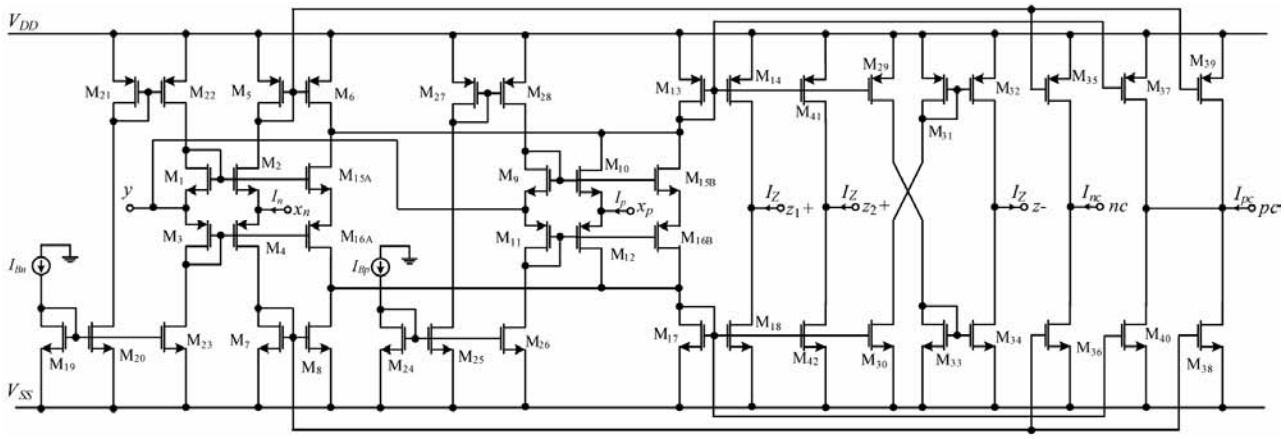

Fig. 2 — Proposed MOS structure of CC-CDCCC

$$R_p \approx \frac{1}{g_{m2} + g_{m4}} \qquad \ldots(2)$$

where g_{m2} and g_{m4} denote the transconductance of M_2 and M_4 transistors, respectively. If M_2 and M_4 are assumed to be matched, then:

$$R_p \approx \frac{1}{\sqrt{8\mu C_{OX}(W/L)I_{Bp}}}. \qquad \ldots(3)$$

Similarly, the intrinsic resistance at x_n terminal which can also be expressed by:

$$R_n \approx \frac{1}{g_{m10} + g_{m12}}. \qquad \ldots(4)$$

Where g_{m10} and g_{m12} denote the transconductance of M_{10} and M_{12} transistors, respectively. If M_{10} and M_{12} are assumed to be matched, then:

$$R_n \approx \frac{1}{\sqrt{8\mu C_{OX}(W/L)I_{Bn}}} \qquad (5)$$

where μ, C_{ox}, W and L are surface mobility, oxide capacitance, channel width and length of MOS transistors (M_2 and M_4) (M_{10} and M_{12}), respectively. It is obvious from Eqs. (3) and (5) that the intrinsic resistances R_p and R_n can be tuned independently through the current bias I_{Bp} and I_{Bn}, respectively.

3 Applications based on Single CC-CDCCC

In this section the low-complexity of two current-mode applications based on single CC-CDCCC and two grounded capacitors are described.

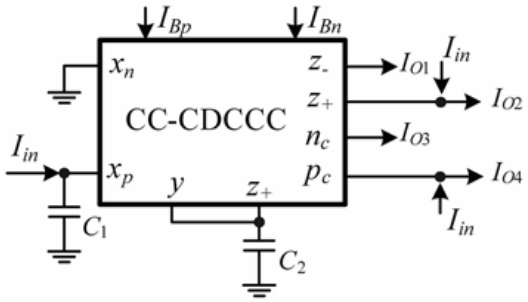

Fig. 3 — Universal filters based on single CC-CDCCC

3.1 Current-mode universal filters based on single CC-CDCCC

The proposed current-mode universal filters based on single CC-CDCCC and two grounded capacitors is shown in Fig. 3. Using routine analysis, four type transfer functions can be obtained from four independent current output terminals i.e. low-pass (LP), high-pass (HP), band-pass (BP) and band-reject (BR). Four current transfer functions can be expressed below:

The BP response $$\frac{I_{O1}}{I_{in}} = \frac{s\left(\frac{1}{R_pC_1}\right)}{D(s)}. \qquad \ldots(6)$$

The BR response $$\frac{I_{O2}}{I_{in}} = \frac{s^2 + \frac{1}{R_nR_pC_1C_2}}{D(s)}. \qquad \ldots(7)$$

The LP response $$\frac{I_{O3}}{I_{in}} = \frac{-\frac{1}{R_nR_pC_1C_2}}{D(s)}. \qquad \ldots(8)$$

The HP response $\frac{I_{O4}}{I_{in}} = \frac{s^2}{D(s)}$. …(9)

where $D(s) = s^2 + s\left(\frac{1}{R_n C_2} - \frac{1}{R_p C_2} + \frac{1}{R_p C_1}\right) + \frac{1}{R_n R_p C_1 C_2}$.

By having an additional z_+ terminal to the CC-CDCCC i.e. output current I_{O5}, and then by summing I_{O2} and I_{O5} the all-pass (AP) response are obtained.

The natural frequency response (ω_0) and quality factor (Q_0) are given by:

$$\omega_0 = \sqrt{\frac{1}{R_p R_n C_1 C_2}} \quad \ldots(10)$$

$$Q_0 = \frac{\sqrt{R_n R_p C_1 C_2}}{R_p C_1 - R_n C_1 + R_n C_2} \quad \ldots(11)$$

Eqs. (10) and (11) show that the parameter ω_0 can be adjusted without disturbing Q_0 by assigning C_1=C_2=C and increasing or decreasing the R_n and R_p simultaneously. Note that the multiple inputs of filter can be obtained by using the additional current buffer circuit. The negative type of multiple outputs current conveyor (MOCC-) in Fig. 4 can be used as a current buffer. Applying the current input (I_{in}), the duplicated current outputs (I_{in1}, I_{in2} and I_{in3}) are obtained at outputs. These duplicated current outputs can be directly applied for the inputs of filter in Fig. 3.

3.2 Current-mode quadrature oscillator based on single CC-CDCCC

The second application is current-mode quadrature oscillator based on single CC-CDCCC and two grounded capacitors is shown in Fig. 5. The output current waveforms are obtained from current output terminals of high impedances; hence no additional buffers are needed.

Characteristic equation can be expressed as:

$$\frac{s}{R_p C_1} = s^2 + s\left(\frac{1}{R_n C_2} - \frac{1}{R_p C_2} + \frac{1}{R_p C_1}\right) + \frac{1}{R_n R_p C_1 C_2} \quad \ldots(12)$$

From Eq. (12), the relations for condition of oscillation (CO) and frequency of oscillation (FO) can be derived:

CO: $R_n = R_p$. …(13)

FO: $\omega_0 = \sqrt{\frac{1}{R_p R_n C_1 C_2}}$ …(14)

It is apparent from Eqs. (13) and (14) that the frequency of oscillation can be tuned electronically by means of varying R_n and R_p simultaneously without affecting the CO.

3.2 Effects of non-idealities and sensitivity analyses of the universal filter and oscillator

Figure 6 shows the simplified equivalent circuit that will be used to represent the behaviour of the non-ideal CC-CDCCC. This mainly results from its finite parasitic elements and non-ideal current transfers. There are parasitic resistances and capacitances (R_y, C_y, and R_z, C_z) from terminals y and z to the ground. It can also be seen that the non-ideal voltage and current transfer characteristic of the CC-CDCCC are given as, $\alpha_p = 1 - \varepsilon_p$, $|\varepsilon_p| \ll 1$ denotes a current tracking error from p to p_c and z terminals,

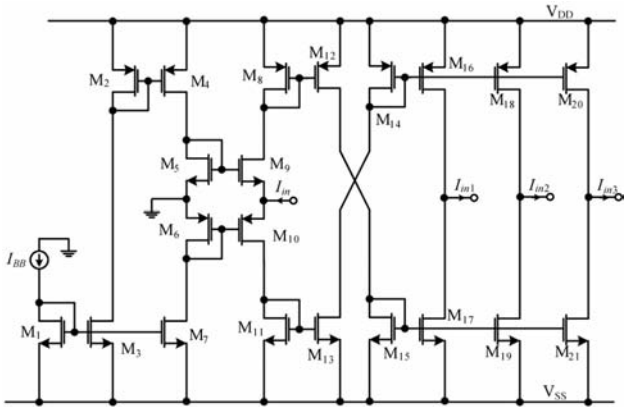

Fig. 4 — Current buffer used for applying in the proposed filter in Fig. 3

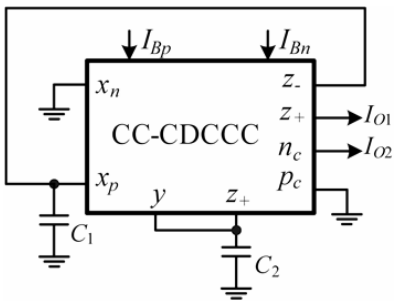

Fig. 5 — Current-mode quadrature oscillator based on single CC-CDCCC

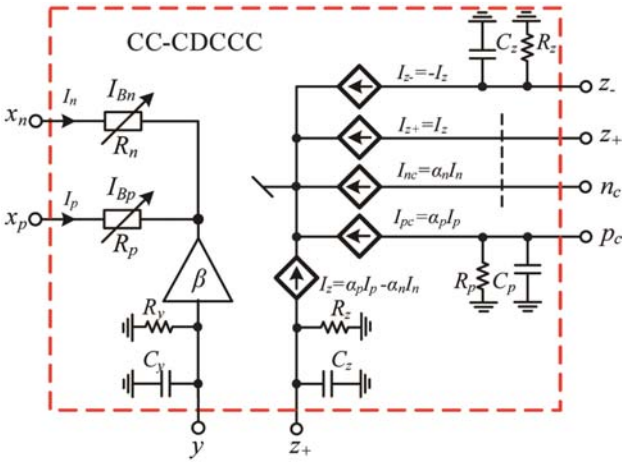

Fig. 6 — Simplified equivalent circuit of the non-ideal CC-CDCCC

$\alpha_n = 1-\varepsilon_n$, $|\varepsilon_n| << 1$ denotes a current tracking error from n to n_c and z terminals, and $\beta = 1-\varepsilon_y$, $|\varepsilon_y| << 1$ denotes a voltage tracking error at y terminal. Taking into account the non-ideal CC-CDCCC characteristics and assuming the value of parasitic resistances at n_c, p_c, y and z terminals are high which can be neglected, the modified current transfer functions of filters in Fig. 3 can be rewritten as:

The BP response

$$\frac{I_{O1}}{I_{in}} = \frac{s\left(\frac{\alpha_p}{R_p C_1}\right)}{D_n(s)} \qquad \ldots(15)$$

The BR response

$$\frac{I_{O2}}{I_{in}} = \frac{s^2 + s\left(\frac{1}{R_p C_1} - \frac{\beta\alpha_p}{R_p C_2'} + \frac{\beta\alpha_n}{R_n C_2'} - \frac{\alpha_p}{R_p C_1}\right) + \frac{\beta\alpha_n}{R_n R_p C_1 C_2'}}{D_n(s)}. \qquad \ldots(16)$$

The LP response

$$\frac{I_{O3}}{I_{in}} = \frac{-\frac{\beta\alpha_n\alpha_p}{R_n R_p C_1 C_2'}}{D_n(s)}. \qquad \ldots(17)$$

The HP response

$$\frac{I_{O4}}{I_{in}} = \frac{s^2 + s\left(\frac{\beta\alpha_p}{R_p C_2'} - \frac{1}{R_p C_1} + \frac{\alpha_p}{R_p C_1} - \frac{\beta\alpha_n}{R_n C_2'}\right) + \frac{\left(\beta\alpha_n\alpha_p - \beta\alpha_n\right)}{R_n R_p C_1 C_2'}}{D_n(s)} \qquad \ldots(18)$$

where

$$D_n(s) = s^2 + s\left(\frac{\beta\alpha_n}{R_n C_2'} - \frac{\beta\alpha_p}{R_p C_2'} + \frac{1}{R_p C_1}\right) + \frac{\beta\alpha_n}{R_n R_p C_1 C_2'}$$

and $C_2' = C_2 + C_y + C_z$. The natural frequency response (ω_{0n}) and quality factor (Q_{0n}) becomes:

$$\omega_{0n} = \sqrt{\frac{\beta\alpha_n}{R_p R_n C_1 C_2'}}. \qquad \ldots(19)$$

$$Q_{0n} = \frac{\sqrt{\beta\alpha_n R_n R_p C_1 C_2'}}{\beta\alpha_n R_p C_1 - \beta\alpha_p R_n C_1 + R_n C_2'}. \qquad \ldots(20)$$

Considering Eqs (19) and (20), it can be seen that the capacitor C_2 has received the influences of parasitic capacitances. In fact, the intrinsic resistances at x_n and x_p terminals (R_n and R_p) are identical. It means that the frequency response and quality factor receive slight effects from the parasitic capacitances, current and voltage tracking errors. In order to reduce these effects, the accurate current mirrors and $C_2 >> C_y + C_z$ are needed. The capacitors C_1 and $C_2 \geq 30$ pF are used to avoid the parasitic capacitance influences. Although Eqs (19) and (20) show that possible deviations in filters parameters could occur due to parasitic impedances of the filters terminals, these deviations could be simply readjusted electronically through R_p and R_n.

The sensitivity analysis with respect to the parameters of the passive elements can be given by:

$$S^{\omega_0}_{\beta,\alpha_n} = -S^{\omega_0}_{C_1,C_2',R_p,R_n} = \frac{1}{2}. \qquad \ldots(21)$$

$$-S^{Q_0}_{C_2',R_n} = S^{Q_0}_{\beta,\alpha_n,C_1,R_p} = \frac{1}{2}. \qquad \ldots(22)$$

It is obvious from Eqs (21) and (22) that all of filters parameter sensitivities in non-ideal case are 0.5 in absolute values and hence, the filters exhibit an attractive sensitivity performance.

Similarly, the non-ideal parameters are taken into account for the oscillator. By using routine analysis, the modified characteristic equation of Fig. 4 yields:

$$s\left(\frac{\alpha_p}{R_p C_1'}\right)=s^2+s\left(\frac{\beta\alpha_n}{R_n C_2'}-\frac{\beta\alpha_p}{R_p C_2'}+\frac{1}{R_p C_1'}\right)+\frac{\beta\alpha_n}{R_n R_p C_1' C_2'} \quad (23)$$

where $C_1'=C_1+C_z$ and $C_2'=C_2+C_y+C_z$. The condition of oscillation and frequency of oscillation become:

$$\text{CO:}\quad \frac{\beta\alpha_n}{R_n C_2'}-\frac{\beta\alpha_p}{R_p C_2'}+\frac{1}{R_p C_1'}-\frac{\alpha_p}{R_p C_1'}=0. \quad \ldots(24)$$

$$\text{FO:}\quad \omega_{0n}=\frac{\beta\alpha_n}{R_n R_p C_1' C_2'}. \quad \ldots(25)$$

Considering Eqs. (24) and (25), it can be seen that the capacitors C_1 and C_2 have received the influence of parasitic capacitances. In fact, the intrinsic resistances at x_n and x_p terminals (R_n and R_p) are identical. It means that the condition of oscillation and frequency of oscillation receive slight effects from the parasitic capacitances, current and voltage tracking errors. In order to reduce these effects, the accurate current mirrors and $C_1>>C_z$, $C_2>>C_y+C_z$ conditions are needed. In this paper, the symmetry structure is implemented for obtaining the identical of x_p and x_n current tracking errors. The capacitors C_1 and $C_2\geq 30$ pF are used to avoid the parasitic capacitance influences.

4 Simulation Results

4.1 Simulation results of the CC-CDCCC characteristics

For the proposed MOS structure of the CC-CDCCC in Fig. 2 all PMOS transistors have the value of W/L equal to 30 µm/0.5 µm whereas for all NMOS transistors 10 µm /0.5 µm except M_1, M_2, M_9, M_{10}, M_{15} use W/L equal to 5 µm/0.35 µm and M_3, M_4, M_{11}, M_{12}, M_{16} use W/L equal to 8 µm/0.35 µm. The voltage supplies are $V_{DD}=-V_{SS}=1.25$ V and the TSMC 0.25 µm SPICE model[27] is used. The total power consumption of the CC-CDCCC is in range from 0.575 µ to 5.75m] W for bias currents $I_{Bp}=I_{Bn}$ in range 0.01-100 µA, respectively. For the additional current buffer in Fig. 4, all PMOS transistors also have the value of W/L equal to 30 µm/0.5 µm whereas for all NMOS transistors 10 µm /0.5 µm except M_5, M_9 use W/L equal to 5 µm/0.35 µm and M_6, M_{10} use W/L equal to 8 µm/0.35 µm. The bias current and supply voltage are 100 µA and ±1.25 V, respectively.

The simulation results of the CC-CDCCC are shown in Figs 7-9 and they show the high performance of this active element. Figure 7 shows the frequency responses of the x_p terminal impedances with varying the bias current I_{Bp} for the following values [0.01, 0.1, 1, 10, 100] µA and then the values of R_p are [43.7 k, 13.8 k, 4.37k , 1.38 k, 437] Ω, respectively. It is evident from Fig. 7 the wide range of R_p tuning. Identical frequency responses of the impedances of x_n terminal are obtained by varying the bias current I_{Bn}. The *dc* characteristics of I_{z+} and I_{z-} against I_p and I_n for I_{Bp}= 100 µA are shown in Fig. 8. It is obvious that the high accuracy and linearity of currents are in the range-100-100µA.

Figures 9 and 10 show the frequency responses of the current transfer of different terminals I_{pc}/I_p, I_{z+}/I_p, I_{z-}/I_p, I_{z+}/I_n, I_{nc}/I_n, and I_{z-}/I_n for $I_{Bp}=I_{Bn}$=100µA. The-

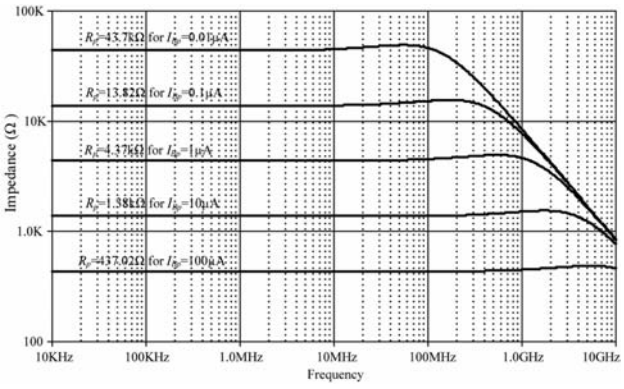

Fig. 7 — Frequency responses of x_p terminal impedances with varying the bias current I_{Bp}

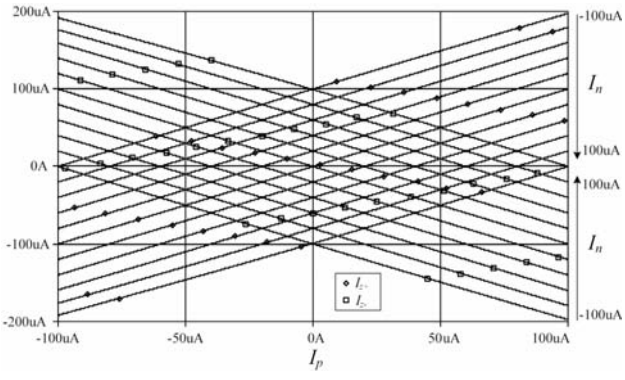

Fig. 8 — dc characteristic of I_{pc},I_{z+} and I_{z-}versus I_p

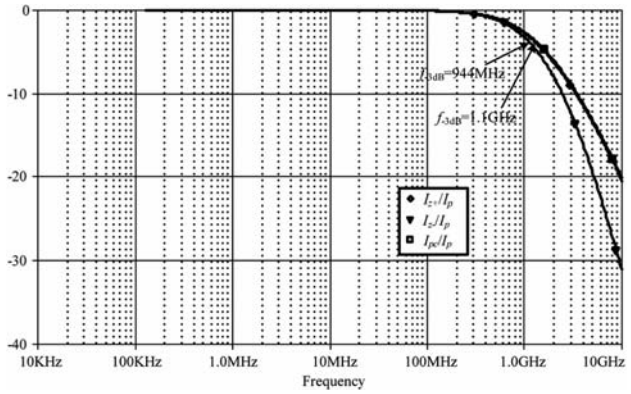

Fig. 9 — Frequency response of I_{pc}, I_{z+} *and* I_{z-}versus I_pc

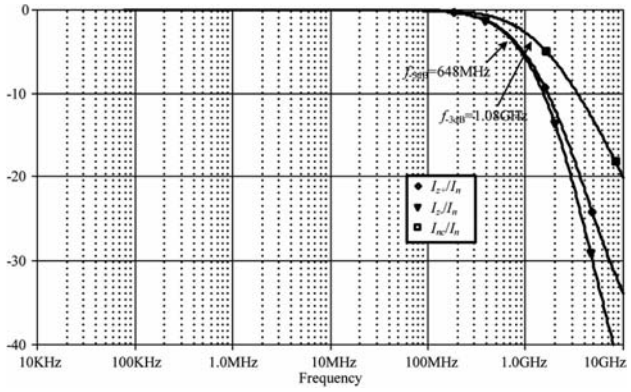

Fig. 10 — Frequency response of I_{nc}, I_{z+} and I_{z-}versus I_n

3dB bandwidths of the current transfers I_{z+}/I_p and I_{z-}/I_p is obtained around 1.1 GHz but I_{pc}/I_p is around 944 MHz. Other results are obtained for the current transfers I_{z+}/I_n, I_{z-}/I_n is obtained around 1.08 GHz but I_{nc}/I_n is around 648 MHz.

Figures 11 and 12 show the total harmonic distortion (THD) of different terminals of proposed CC-CDCCC. Sinusoidal 10 MHz are applied at I_p and I_n with bias currents I_{Bn}=I_{Bp}=100 μA. It is obvious that the THD results of different terminals are lower than 1% under the 100 μA input current amplitude.

4.2 Simulation results of the universal filters

The simulations of the proposed universal filters are shown in Figs 13-15. Figure 13 shows the current-mode magnitude responses of LP, HP, BP and BR when C_1=C_2= 30 pF and R_p= R_n= 437.02 Ω (for I_{Bp}=I_{Bn}= 100 μA). The simulated natural frequency f_0= 12.023 MHz and the theoretical one f_0= 12.139 MHz.

The electronic tunable facility for a wide range of frequencies of the filter are shown on BP responses

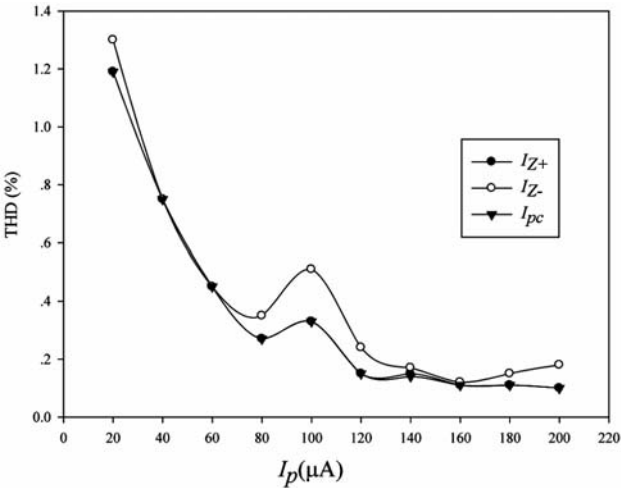

Fig. 11 — THD of I_{Z+}, $I_{Z-}$and I_{pc} by applying the sinusoidal 10 MHz at I_p with bias currents I_{Bn}=I_{Bp}=100 μA

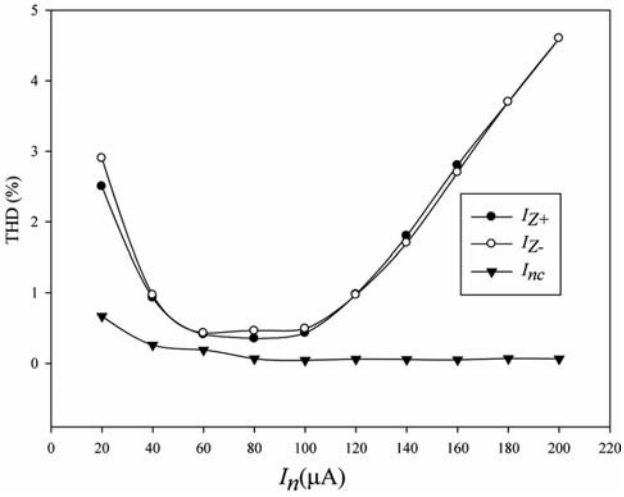

Fig. 12 — THD of I_{Z+}, I_{Z-} and I_{nc} by applying the sinusoidal 10 MHz at I_p with bias currents I_{Bn}=I_{Bp}=100 μA

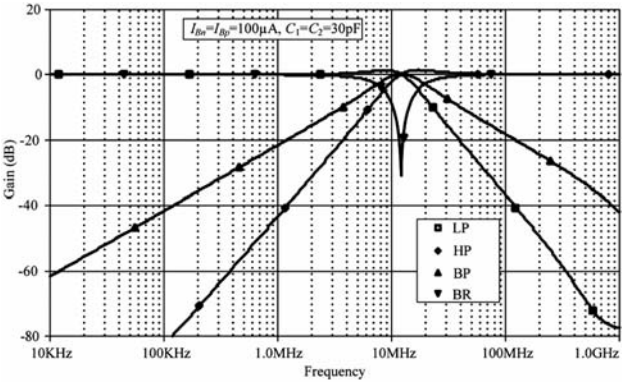

Fig. 13 — Current-mode magnitude responses of *LP, HP, BP* and *BR*

for C_1= C_2= 30 pF in Fig. 14 by stepping the bias currents I_{B1}=I_{B2}= [0.01, 0.1, 1, 10, 100] µA. The cutoff frequencies are in range from 120 kHz to 12 MHz which prove the capability of tunability in wide range of frequencies. The current-mode magnitude and phase response of AP with C_1= C_2= 30 pF are shown in Fig. 15. The simulated natural frequency f_0= 12.05 MHz and the theoretical one f_0= 12.139 MHz. The comparison of proposed filter with previous filter is listed in Table 1. The proposed CC-CDCCC can provide tunable second-order filter without the resistors by using only 44 transistors.

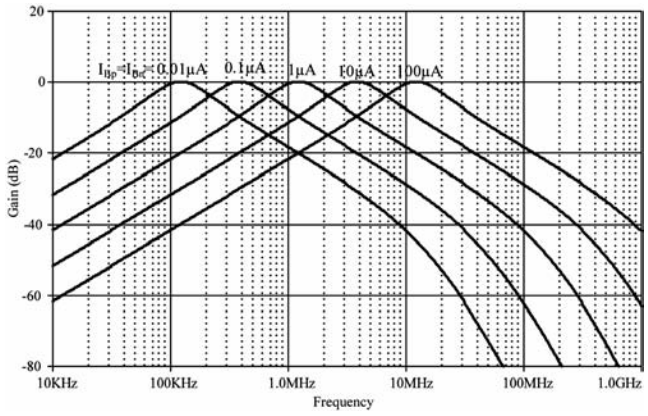

Fig. 14 — Band-pass responses with C_1= C_2= *30* pF and varying the bias currents I_{Bp}=I_{Bn}

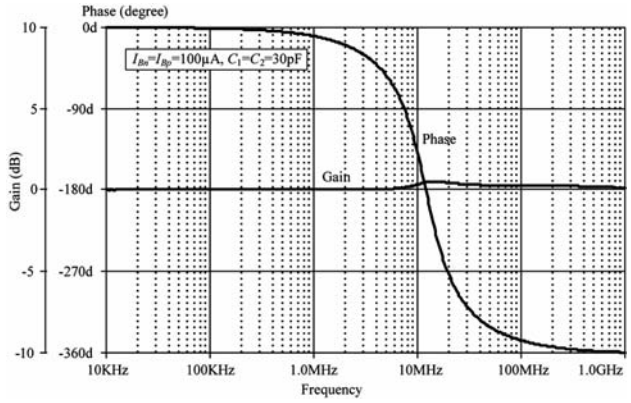

Fig. 15 — Current-mode magnitude and phase responses of AP with C_1= C_2= *30 pF*

4.3 Simulation results of quadrature oscillator

The simulations of the proposed quadrature oscillator are shown in Figs 16 and 17. Figure 16 shows the current output waveforms I_{o1} and I_{o2} when C_1= C_2= 30 pF. To ensure that the oscillations would start the value of R_p is adjusted slightly lower than R_n i.e. R_p =435.935 Ω (I_{Bp}= 100.5 µA) and R_n =437.02 Ω (I_{Bn}= 100 µA). The simulated frequency f =12.203 MHz and the theoretical one f =12.139 MHz. The spectrum of oscillator output currents is shown in Fig. 17. The total harmonic

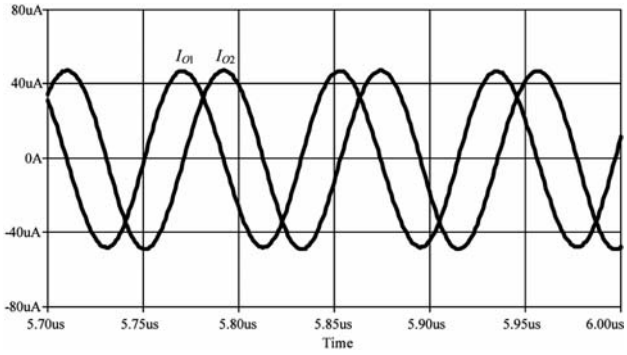

Fig. 16 — Waveforms of the oscillator output currents

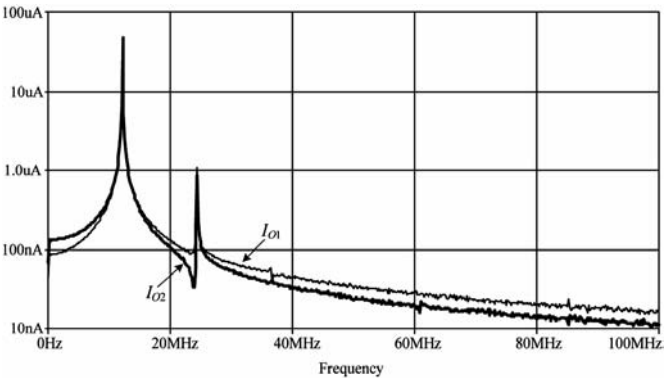

Fig. 17 — Spectrum of oscillator output currents

Table1 — Comparison features of proposed filter with previous filters

	Active element	Transistors	Bandwidth	Electronic tuning	External resistors	Technology
[6]	3 DVCCs	54	<10 MHz	no	4	TSMC 0.35 µm
[7]	3ICCIIs	54	<10 MHz	no	2	TSMC 0.18 µm
[8]	3 DVCCs	60	<10 MHz	yes	no	TSMC 0.35 µm
[9]	1 CDTA	23	<10 MHz	Yes	3	BJT ALA400
[11]	2 CCCIIs	78	<10 MHz	Yes	no	BJT ALA400
Proposed	1 CC-CDCCC	44	>10 MHz	Yes	no	TSMC 0.25 µm

Table 2 — Comparison features of proposed quadrature oscillator with previous quadrature oscillators

	Active element	Transistors	Bandwidth	Electronic tuning	External resistors	Technology
[16]	2 CDTAs	48	<10 MHz	No	2	MIETEC 0.5 µm
[17]	1 CDTA	23	<10 MHz	Yes	1	0.7 µm
[19]	1 CFTA+ 1 UGVF	>20	<1 MHz	Yes	2	BJT ALA400
[22]	3 CCIIs	39	<1 MHz	No	3	AD844
[25]	2 CDTAs	48	<10 MHz	Yes	1	MIETEC 0.5 µm
Proposed	1 CC-CDCCC	44	>10 MHz	Yes	No	TSMC 0.25 µm

distortion (THD) of the current output waveforms I_{o1} and I_{o2} is 2.33 % and 1.87 %, respectively. The comparison of proposed quadrature oscillator with previous quadrature oscillator is listed in Table 2. The proposed CC-CDCCC can provide tunable quadrature oscillator without the resistors by using only 44 transistors.

5 Conclusions

A new high performance electronically tunable active element CC-CDCCC is presented in this paper. The main features of this element are large dynamic range, wide bandwidth and high accuracy. Furthermore, its intrinsic resistances of the input current terminals can be independently set by external balancing bias currents. Based on this active element, a current-mode universal filters and quadrature oscillator are presented as possible applications. Both applications are electronically controlled for wide range of frequencies and they employ only single CC-CDCCC and two grounded capacitors which are advantageous for monolithic integration. The simulation results proved the high performance of the proposed circuit and correspondence with theory. The total power consumption of the CC-CDCCC device is lower than 5.75mW.

Acknowledgement

The authors would like to thank Faculty of Engineering, King Mongkut's Institute of Technology Ladkrabang for their supports.

The described research was also performed in laboratories supported by the SIX project; the registration number CZ.1.05/2.1.00/03.0072. The operational program Research and Development for Innovation has been supported by Czech Science Foundation project No.: P102-14-07724S.

References

1 Fabre A, Saaid O, Wiest F &Boucheron C,*Electron. Lett*, 31 (1995) 1727.
2 Prommee P &Somdunyakanok M,-*IntJ Electron Commun(AEU)*, 65 (2011) 1.
3 Herencsar N, Koton J, Vrba K, Lahiri A &Cicekoglu O, *Int. Conf. Applied Electronics*, Plzeň: University of West Bohemia, (2010) pp 121.
4 Jaikla W &Prommee P, *Radioengineering*, 20 (2011) 594.
5 Tangsrirat W, Prasertsom D, Piyatat T &Surakampontorn W, *Int J Electron*, 95(2008) 1119.
6 Horng J W, Hou C L, Chang C M, Chou H P & Lin C T,*Circuits Syst. Signal Process*, 25 (2006) 767.
7 Horng J W, *Indian J Pure & Appl Phys*, 49 (2011) 214.
8 Minaei S & Ibrahim M A, *Int J Circ Theor Appl*, 37 (2009) 793.
9 Prasad D, Bhaskar D R & Singh A K, *Analog Integr Circ Sig Process*, 61 (2009) 309.
10 Kumngern M, Torteanchai U & Dejhan K, *Radioengineering*, 20 (2011) 327.
11 Kumngern M, Jongchanavawat W & Dejhan K, *Int J Electron*, 97 (2010) 511.
12 Tangsrirat W, Kritsada B,*Indian J Pure & ApplPhys*, 50 (2012) 133.
13 Biolek D, Senani R, Biolkova V & Kolka Z, *Radioengineering*, 17:4 (2008) 15.
14 Abrishafimar A, Karimi Y &Navidi M M, *IEICE Electronics Express*, 9 (2012) 104.
15 Prommee P, Dejhan K, *Int J Electron*, 89 (2002) 365.
16 Keskin A Ü & Biolek D, *IEE Proc.-Circuits Devices Syst.*, 153 (2006) 214.
17 Jaikla W, Siripruchyanun M, Bajer J & Biolek D, *Radioengineering*, 17:4 (2008) 33.
18 Biolek D, Lahiri A, Jaikla W, Siripruchyanun M &Biolkova V, *Microelectronics Journal*, 42 (2011) 1116.
19 Herencsár N, Vrba K, Koton J & Lahiri A, *Int J Electron*, 97 (2010) 897.
20 Horng J W, *IEICE Transactions on Fundamentals of Electronics*, E86-A (2003) 2152.
21 Horng J W, Hou C L, Chang C M, Chou H P, Lin C T & Wen Y H,*ETRI Journal*, 28 (2006) 486.
22 Horng J W,*Computers and Electrical Engineering*, 31 (2005) 81.
23 Herencsár N, Koton J, Vrba K & Lahiri A, *IEICE Electronics Express*, 6 (2009) 1708.
24 Lahiri A, *Analog Integr. Circuits Signal Process*, 61 (2009) 199.
25 Kumngern M, Lamun P & Dejhan K, *Int J Electron*, 99 (2012) 971.
26 Bruun E, *Int J Electron*, 74 (1993) 93.
27 Prommee P, Angkeaw K, Somdunyakanok M & Dejhan K, *Analog Integr Circuits Signal Process*, 61 (2009) 93.